

Stereochemical studies of cobalt ethylenediamine complexes and their tetrathionate salts: Interactions between complex configuration and tetrathionate conformation

Meritxell Casadesus, Michael P. Coogan^{*}, Elenna Davies, Li-ling Ooi

Department of Chemistry, Cardiff University, Cardiff CF10 3AT, Cymru/Wales, UK

Received 29 March 2007; received in revised form 4 June 2007; accepted 8 June 2007

Available online 30 June 2007

Abstract

A range of chiral coordination complexes of the formulae *cis*-[Co(en)2XY] where X, Y = hal, NH₃, NO₂, ox, SCN have been prepared as the halide or pseudohalide salts, and the novel examples have been structurally characterised and their stereochemical behaviour studied. Salt metathesis of certain of these species to the corresponding tetrathionates is described, and the tetrathionates structurally characterised and the stereochemical relationship between the conformations of the chiral complexes and the pseudochiral tetrathionates analysed. The patterns of cation–cation and cation–anion interactions are discussed in the context of the reported ability of the tetrathionate ion to induce conglomerate crystallisation in such species, and tetrathionate chirality in the literature.

© 2007 Elsevier B.V. All rights reserved.

Keywords: Cobalt; Stereochemistry; Werner complexes; Conglomerate crystallisation

1. Introduction

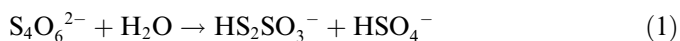
There is great practical and philosophical interest in the spontaneous resolution of racemic material by conglomerate crystallisation. Conglomerate crystallisation is the phenomenon whereby a sample of racemic material spontaneously crystallises as a physical mixture of enantiomorphic crystals, as opposed to a racemate in which each crystal contains both enantiomers [1]. Conglomerate crystallisation provides a means for the amplification of chirality in a sample of low e.e. as the first formed crystals, necessarily of a single enantiomer, may act as seeds, encouraging further crystallisation only of that enantiomer. In the case of a solution in which the enantiomers are equilibrating (i.e. the sample is constantly racemising), conglomerate crystallisation may provide a mechanism for an ‘asymmetric transformation of the second kind’ [2] which can allow the conversion of a racemic sample to a single enantiomer in high yield. In addition to the prac-

tical applications in asymmetric synthesis, the possibility of linking conglomerate crystallisation and asymmetric transformation with photochemical deracemisation would be particularly interesting as this could provide a model for the origin of biological homochirality [3,4]. Circularly polarised light has been shown to be capable of photochemically deracemising certain species, however, the e.e. obtained is always low, and a mechanism for chiral amplification (e.g. fractional conglomerate crystallisation) is required if this is to be proposed as a possible model for the origin of prebiotic chirality induced by circularly polarised cosmic radiation [5]. It is known that many cobalt diamine complexes may be photochemically racemised [6], and there is a family of such complexes [Co(en)2XY] + Z⁻ (themselves significant in the history of stereochemistry of coordination chemistry) which contains examples which crystallise as conglomerates, so an investigation of these species was undertaken. The earliest examples of chiral coordination complexes were of the type [Co(en)2NH3Hal] + Hal⁻, (Hal = Cl, Br) **1a,b** which were prepared and resolved by Werner himself [7]. Werner and students also prepared cobalt ethylene diamine complexes

^{*} Corresponding author. Tel.: +44 2920874066; fax: +44 2920874030.
E-mail address: cooganmp@cf.ac.uk (M.P. Coogan).

which display conglomerate crystallisation, in particular the nitrito species [Co(en)₂(NO₂)₂] Hal- **2a,b** crystallise as conglomerates [8a,9a], and were amongst the first examples known of conglomerate crystallisation of coordination complexes, although Werner originally missed the conglomerate crystallisation of these complexes and noted only their molecular chirality.

More recently, Bernal has studied the conglomerate crystallisation of a vast series of coordination complexes [9] including many related species, and has pointed out the usefulness of the tetrathionate ion **3** as a conglomerating agent for ethylene diamine complexes of transition metals, including the tetrathionate analogue obtained by salt metathesis of **1b** [9c]. The tetrathionate ion is particularly interesting as it can take up enantiomeric conformations around the axis formed by the mutual angles between the S–S–S–S bonds, and thus allows chiral recognition between enantiomeric cations and anions, encouraging conglomerate crystallisation [9c]. One complication with the use of these species is the slow spontaneous equilibration between ions in solution [9g]:



which has led to the observation of bisulphate salts formed by cleavage of S–S bonds, however, this appears to cause complications only in a minority of cases.

As a general class then, it appears that Werner-type complexes of cobalt [9a,9b,9c,9d] and other metals [9e] are suitable and popular target in the ongoing search for new conglomerate species, and the chances of conglomerate formation are increased by substituents and counterions which allow hydrogen bonding, and in particular by the use of the tetrathionate anion. Although, we are far from being at the stage of predicting conglomerate formation, or accurately designing systems which will crystallise as conglomerates, cobalt amine complexes and their tetrathionate salts, therefore were an attractive series of compounds to study crystallisation and hydrogen bonding patterns.

2. Experimental

2.1. General experimental

All starting materials and reagents were purchased from commercial suppliers and used as supplied unless otherwise stated. Full characterisation (¹H, ¹³C, IR, MS, and CHN) has been attempted for novel compounds; literature materials which have previously only been crystallographically characterised are characterised by at least two bulk techniques to validate the resynthesis. NMR spectra were recorded on a Bruker DPX 400 MHz at 400 MHz (proton) and 160 MHz (carbon), or an APX 250 at 250 MHz and 100 MHz, respectively. Amino group integrations are reported as fractions in cases where exchange with D₂O

occurred. Melting points were recorded on a Kopfler hot stage and are uncorrected. IR spectra were recorded on a Perkin Elmer 1600 FT IR as thin films or nujol mulls; mass spectra were recorded on a VG Fisons Platform II or at the EPSRC national mass spectrometry service in Swansea (HRMS). Elemental analyses were performed by Warwick Analytical Services (University of Warwick). Tetrathionate starting materials were synthesised according to the literature methods [9].

2.2. Crystal data

Crystal data for 1b: C₄H₁₉Br₃CoN₅, *M* = 435.90, red block, 0.20 × 0.20 × 0.15 mm³, monoclinic, space group *P*2₁/*n* (no. 14), *a* = 7.6301(2), *b* = 12.3587(4), *c* = 13.9682(5) Å, β = 98.5640(10)°, *V* = 1302.49(7) Å³, *Z* = 4, *D*_c = 2.223 g/cm³, *F*₀₀₀ = 840, KappaCCD, Mo Kα radiation, λ = 0.71073 Å, *T* = 150(2) K, 2θ_{max} = 55.0°, 11930 reflections collected, 2910 unique (*R*_{int} = 0.0950). Final GooF = 1.038, *R*₁ = 0.0457, *wR*₂ = 0.0870, *R* indices based on 2035 reflections with *I* > 2σ(*I*) (refinement on *F*²), 119 parameters, 0 restraints. μ = 10.492 mm⁻¹.

Crystal data for 6: C₄H₁₉CoI₄N₅, *M* = 703.77, black block, 0.20 × 0.20 × 0.20 mm³, triclinic, space group *P*1̄ (no. 2), *a* = 7.9760(2), *b* = 8.4940(2), *c* = 13.5110(5) Å, α = 93.6490(10), β = 104.4510(10), γ = 111.1420(10)°, *V* = 814.67(4) Å³, *Z* = 2, *D*_c = 2.869 g/cm³, *F*₀₀₀ = 634, Mo Kα radiation, λ = 0.71073 Å, *T* = 293(2) K, 2θ_{max} = 55.0°, 14911 reflections collected, 3711 unique (*R*_{int} = 0.1265). Final GooF = 0.887, *R*₁ = 0.0445, *wR*₂ = 0.1224, *R* indices based on 3149 reflections with *I* > 2σ(*I*) (refinement on *F*²), 140 parameters, 0 restraints. μ = 8.614 mm⁻¹.

Crystal data for 8: C₄H₁₈ClCoN₆O₅, *M* = 324.62, yellow block, 0.25 × 0.25 × 0.20 mm³, monoclinic, space group *P*2₁/*n* (no. 14), *a* = 7.2606(3), *b* = 11.9473(4), *c* = 14.0218(6) Å, β = 95.7830(10)°, *V* = 1210.12(8) Å³, *Z* = 4, *D*_c = 1.782 g/cm³, *F*₀₀₀ = 672, KappaCCD, Mo Kα radiation, λ = 0.71073 Å, *T* = 150(2) K, 2θ_{max} = 54.9°, 8214 reflections collected, 2748 unique (*R*_{int} = 0.0569). Final GooF = 1.049, *R*₁ = 0.0345, *wR*₂ = 0.0698, *R* indices based on 2208 reflections with *I* > 2σ(*I*) (refinement on *F*²), 154 parameters, 0 restraints. μ = 1.661 mm⁻¹.

Crystal data for 9: C₈H₃₂Co₂N₁₂O₁₄S₄, *M* = 766.56, yellow block, 0.50 × 0.45 × 0.13 mm³, monoclinic, space group *P*2₁/*a* (no. 14), *a* = 12.4425(2), *b* = 7.79690(10), *c* = 27.6488(5) Å, β = 92.3300(10)°, *V* = 2680.07(7) Å³, *Z* = 4, *D*_c = 1.900 g/cm³, *F*₀₀₀ = 1576, KappaCCD, Mo Kα radiation, λ = 0.71073 Å, *T* = 150(2) K, 2θ_{max} = 55.0°, 15938 reflections collected, 5959 unique (*R*_{int} = 0.0693). Final GooF = 1.020, *R*₁ = 0.0452, *wR*₂ = 0.1076, *R* indices based on 4704 reflections with *I* > 2σ(*I*) (refinement on *F*²), 361 parameters, 0 restraints. μ = 1.634 mm⁻¹.

Crystal data for 10: C₄H₂₁ClCoN₅O₇S₄, *M* = 473.88, pink plate, 0.28 × 0.20 × 0.05 mm³, monoclinic, space group *P*2₁/*n* (no. 14), *a* = 11.9042(4), *b* = 9.5176(4), *c* = 15.2284(5) Å, β = 101.993(2)°, *V* = 1687.71(11) Å³, *Z* = 4, *D*_c = 1.865 g/cm³, *F*₀₀₀ = 976, KappaCCD, Mo Kα

radiation, $\lambda = 0.71073 \text{ \AA}$, $T = 150(2) \text{ K}$, $2\theta_{\text{max}} = 54.9^\circ$, 9915 reflections collected, 3859 unique ($R_{\text{int}} = 0.0895$). Final GooF = 1.062, $R_1 = 0.0509$, $wR_2 = 0.1204$, R indices based on 2981 reflections with $I > 2\sigma(I)$ (refinement on F^2), 209 parameters, 0 restraints. $\mu = 1.707 \text{ mm}^{-1}$.

Crystal data for 12: $\text{C}_{12}\text{H}_{48}\text{Co}_2\text{N}_8\text{O}_{21.50}\text{S}_4$, $M = 894.68$, red block, $0.30 \times 0.25 \times 0.10 \text{ mm}^3$, triclinic, space group $P\bar{1}$ (no. 2), $a = 11.7530(3)$, $b = 12.5463(3)$, $c = 13.2064(3) \text{ \AA}$, $\alpha = 68.1750(10)$, $\beta = 89.7030(10)$, $\gamma = 73.3970(10)^\circ$, $V = 1721.21(7) \text{ \AA}^3$, $Z = 2$, $D_c = 1.726 \text{ g/cm}^3$, $F_{000} = 932$, KappaCCD, Mo $K\alpha$ radiation, $\lambda = 0.71073 \text{ \AA}$, $T = 150(2) \text{ K}$, $2\theta_{\text{max}} = 55.2^\circ$, 30114 reflections collected, 7871 unique ($R_{\text{int}} = 0.1149$). Final GooF = 1.076, $R_1 = 0.0565$, $wR_2 = 0.1300$, R indices based on 6454 reflections with $I > 2\sigma(I)$ (refinement on F^2), 433 parameters, 6 restraints. $\mu = 1.298 \text{ mm}^{-1}$.

Crystal data for 13: $\text{C}_8\text{H}_{32}\text{Cl}_4\text{Co}_2\text{N}_8\text{O}_6\text{S}_4$, $M = 724.32$, green block, $0.30 \times 0.25 \times 0.10 \text{ mm}^3$, triclinic, space group $P\bar{1}$ (no. 2), $a = 9.1266(2)$, $b = 12.0312(3)$, $c = 12.6384(4) \text{ \AA}$, $\alpha = 79.7030(10)$, $\beta = 87.0570(10)$, $\gamma = 71.353(2)^\circ$, $V = 1293.70(6) \text{ \AA}^3$, $Z = 2$, $D_c = 1.859 \text{ g/cm}^3$, $F_{000} = 740$, KappaCCD, Mo $K\alpha$ radiation, $\lambda = 0.71073 \text{ \AA}$, $T = 150(2) \text{ K}$, $2\theta_{\text{max}} = 54.9^\circ$, 23057 reflections collected, 5897 unique ($R_{\text{int}} = 0.1131$). Final GooF = 1.028, $R_1 = 0.0578$, $wR_2 = 0.1080$, R indices based on 3591 reflections with $I > 2\sigma(I)$ (refinement on F^2), 295 parameters, 6 restraints. $\mu = 2.060 \text{ mm}^{-1}$.

2.3. Synthetic procedures

2.3.1. Synthesis of *cis*-[CoCl₂(en)₂]Cl [16]

The synthesis was performed following a procedure similar to that described in the literature [15]. In a 250 mL beaker, 60 mL (90 mmol) of a 10% solution of ethylenediamine was added to a solution of 16 g (67 mmol) of $\text{CoCl}_2 \cdot 6\text{H}_2\text{O}$ in 50 mL of water. A stream of air was passed through the solution for 7.5 h and then the system was left open to the air overnight. 35 mL of conc. HCl was added and the solution was concentrated to ca. 75 mL, collecting afterwards by filtration a green solid: *trans*-[CoCl₂(en)₂]Cl. The later, after being washed with ethanol and ether, was dried at 110 °C until no more acid vapours were noticed (testing with dampened pH indicator paper). The residue was dissolved in 50 mL of water and it was evaporated until dryness in a silicon bath to finally obtain 6.82 g (53%) of *cis*-[CoCl₂(en)₂]Cl [16]. δH (400 MHz, D₂O): 2.39, m, 2H, CH₂; 2.63, m, 4H, CH₂; 2.86, m, 2H, CH₂; 5.19, s, 2H, NH₂; 5.35, s, 2H, NH₂; 5.58, s, 2H, NH₂; 5.85, s, 2H, NH₂. ν_{max} 3426 cm⁻¹, 3187 cm⁻¹, 1635 cm⁻¹, 1569 cm⁻¹.

2.3.2. Synthesis of *cis*-[CoCl(NH₃)(en)₂]Cl₂ (1a) [9c]

This synthesis was performed following a similar procedure to that described in the literature [9c]. To a 25 mL round bottom flask were added 2.56 g (3.19 mmol) of [(H₂O)₂Co{(OH)₂Co(en)₂}₂](SO₄)₂ · 5H₂O (4) [10] and 6.8 mL of H₂O. 3.75 g (70 mmol) of NH₄Cl was then added and the mixture was stirred for 1 min at room temperature,

followed by 5 min stirring at 50 °C. Immediately after the stirring had finished, the mixture was cooled down in an ice bath for 1 h. The solid was collected by filtration, washed with ethanol and ether to obtain 0.44 g (46%) of *cis*-[CoCl(NH₃)(en)₂]Cl₂ (1a) [9c]. δH (400 MHz, D₂O) 2.45, m, 2 H, CH₂; 2.66, m, 4H, CH₂; 2.83, m, 2H, CH₂; 3.37, s, 0.1H, NH₃; 5.04, s, 0.1H, NH₂; 5.18, s, 0.1H, NH₂; 5.22, s, 0.1H, NH₂; 5.40, 2, 0.1H, NH₂. δC (101 MHz, D₂O): 44.44, 44.81, 45.05, 45.17. M.p. 246–248 °C. ν_{max} 3430 cm⁻¹, 3287 cm⁻¹, 3237 cm⁻¹. m/z (ES): theoretical isotope model for C₄H₁₉Cl₂CoN₅: 336.0 (78.3%); 338.0 (100%); 340.0 (47.9%); 432.0 (10.8%). Observed data: 336.0 (66.2%); 338.1 (100%); 340.1 (43.2%); 432.0 (10.8%).

2.3.3. Synthesis of *cis*-[CoBr(NH₃)(en)₂]Br₂ (1b) [12]

This synthesis was performed following a similar procedure to that described in the literature [12]. To a 50 mL round bottom flask was added 2.56 g (3.19 mmol) of [(H₂O)₂Co{(OH)₂Co(en)₂}₂](SO₄)₂ · 5H₂O 4[10] and 6.8 mL of H₂O. 6.86 g (70 mmol) of NH₄Br were then added and the mixture was stirred for 1 min at room temperature, followed by 5 min stirring at 50 °C. Immediately after the stirring had finished, the mixture was cooled down in an ice bath for 1 h. The product was recrystallised from 5% HBr to obtain 1.58 g (57%) of dark violet crystals *cis*-[CoBr(NH₃)(en)₂]Br₂ (1b) [12]. δH (400 MHz, D₂O) 2.22, m, 2H, CH₂; 2.49, m, CH₂, 4H; 2.71, m, 2H, CH₂; 3.16 s, 3H, NH₃; 4.00, s, 1H, NH; 4.07, s, 1H, NH; 4.29, s, 1H, NH; 4.51, s, 1H, NH; 4.88, s, 1H, NH; 4.98, s, 2H, NH; 5.18, s, 1H, NH. δC (101 MHz, D₂O): 44.70; 45.05; 45.17; 45.33; 45.46. m.p.: 225–227 °C. m/z (ES): theoretical isotope model for C₄H₁₆Br₂CoN₄: 336.9 (51.3%); 338.9 (100%); 340.9 (48.6%), observed data: 336.9 (47.3%); 339.0 (100%); 341.0 (47.3%). ν_{max} 3413 cm⁻¹, 3217 cm⁻¹.

2.3.4. Synthesis of *cis*-[Co(NO₂)₂(en)₂]Cl (2a) [9a]

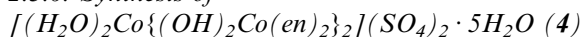
The synthesis was performed following the procedure described in the literature [9a]. 2.85 g (10 mmol) of *cis*-[CoCl₂(en)₂]Cl and 1.5 g (22 mmol) of NaNO₂ were dissolved in the minimum amount of hot (60 °C) water. The mixture was stirred for 1 h at 60 °C, then cooled down in an ice bath for 2 h. The product was collected by filtration and recrystallised from water, to finally give 0.460 g (15%) of *cis*-[Co(NO₂)₂(en)₂]Cl (2a) [9a]. δH (400 MHz, D₂O) 2.52, m, 2H, CH₂; 2.59, m, 4H, CH₂; 2.69, m, 2H, CH₂; 4.25, s, 0.1H, NH₂; 4.42, s, 0.1H, NH₂; 5.26, s, 0.1H, NH₂. δC (101 MHz, D₂O) 43.67; 45.39. M.p.: Decomposes at 228 °C. m/z (ES): theoretical isotope model for C₄H₁₆CoN₆O₄: 271.1 (100%); 272.1 (7.4%). Observed data: 271.1 (100%); 272.1 (7.4%).

2.3.5. Synthesis of *cis*-[Co(NO₂)₂(en)₂]Br (2b) [9a]

The synthesis was performed using a procedure similar to that described in the literature [9a]. To a 50 mL round bottom flask were added 0.85 g (10 mmol) of NaNO₂ and 2 mL of water at 50 °C. The solution was stirred until

everything was dissolved and then *cis*-[CoBr(NH₃)(en)₂]Br₂ was added. The mixture was stirred at 50 °C for 1 h, followed by cooling down in an ice-bath. Orange-yellow solid was collected by filtration to give 0.274 g (39%) of *cis*-[Co(NO₂)₂(en)₂]Br (**2b**) [9a]. δH (400 MHz, D₂O) 2.52, m, 2H, CH₂; 2.59, m, 4H, CH₂; 2.68, m, 2H, CH₂; 4.25, s, 0.1H, NH₂; 4.40, s, 0.1H, NH₂; 4.90, s, 0.1H, NH₂; 5.25, s, 0.1H, NH₂. δC (101 MHz, D₂O) 43.65; 45.37. M.p.: decomposes at 211 °C. ν_{max} 3096 cm⁻¹, 1584 cm⁻¹, 1556 cm⁻¹. *m/z* (ES) Theoretical isotope model for C₄H₁₆CoN₆O₄: 271.1 (100%); 272.1 (7.4%). Observed data: 271.1 (100%); 272.1 (6.7%).

2.3.6. Synthesis of



This synthesis was performed following a similar procedure to that described in the literature [17]. To a 500 mL round bottom flask were added 145 g (516 mmol) of CoSO₄ · 7H₂O and 300 mL (450 mmol) of a 10% solution of ethylenediamine in water. The mixture was stirred for 4 h, then allowed to rest for 1 h and finally filtered. The mother liquids were left to crystallize for one night, before filtering to obtain 20.71 g (22.9%) of [(H₂O)₂Co{(OH)₂Co(en)₂}]₂(SO₄)₂ · 5H₂O [10]. ν_{max} : 3416 cm⁻¹, 3247 cm⁻¹, 3116 cm⁻¹. *m/z* Expected ions not found by ESI or MALDI.

2.3.7. Synthesis of *cis*-[CoI(NH₃)(en)₂]I₃ (**6**)

This synthesis was performed following a similar procedure to that for *cis*-[CoBr(NH₃)(en)₂]Br₂. To a 50 mL round bottom flask were added 2.56 g (3.19 mmol) of [(H₂O)₂Co{(OH)₂Co(en)₂}]₂(SO₄)₂ · 5H₂O **4** and 6.8 mL of H₂O. 10.15 g (70 mmol) of NH₄I was then added and the mixture was stirred for 1 min at room temperature, followed by 5 min stirring at 50 °C. Immediately after that the mixture was cooled down in an ice bath for 1 h. After filtration of much green-grey solid, the mother liquid was left to crystallize. After several days of crystallization the solution was filtered and washed with cold water to give 0.184 g (16.4%) of dark red *cis*-[CoI(NH₃)(en)₂]I₃ (**6**). δH (400 MHz, D₂O) 2.40, m, 2H, CH₂; 2.73, m, 4H, CH₂; 2.99, m, 2H, CH₂; 4.57, s, 0.1H, NH₂; 4.90, s, 0.1H, NH₂; 5.24, s, 0.1H, NH₂. M.p.: decomposes at 206 °C. ν_{max} : 3182 cm⁻¹, 3096 cm⁻¹. *m/z*: expected ions were not found by FAB or ESI. C₄H₁₉N₅CoI₄ requires: C, 6.83; H, 2.72; N, 9.63. Found: C, 6.78; H, 2.62; N, 9.95%.

2.3.8. Synthesis of *trans*-[Co(NCS)₂(en)₂]NCS (**7**)

This synthesis was carried out using a variation on the method for *cis*-[CoBr(NH₃)(en)₂]Br₂. To a 50 mL round bottomed flask were added 2.6 g (3.2 mmol) of [(H₂O)₂Co{(OH)₂Co(en)₂}]₂(SO₄)₂ · 5H₂O **4**, 5.3 g (70 mmol) of NH₄SCN and 6.8 mL of H₂O. The mixture was stirred for 1 min at room temperature and then was stirred for 5 min at 50 °C. After that the mixture was cooled down in an ice bath for 2 h and as the bath warmed to room temperature it was left crystallizing overnight. The solid was

collected by filtration to obtain 0.179 g (8%) of *trans*-[Co(NCS)₂(en)₂]NCS **7**. $^{14}\delta\text{H}$ (400 MHz, D₂O) 2.59, s, 8H, CH₂. δC (101 MHz, D₂O) 45.43; 45.72; 141.23. M.p.: 226–228 °C. ν_{max} 3216 cm⁻¹, 2107 cm⁻¹.

2.3.9. Synthesis of *cis*-[Co(NO₂)₂(en)₂]S₄O₆ (**9**)

The synthesis was carried out according to a variation on the literature procedure for similar systems [9a]. To 0.306 g (1 mmol) of *cis*-[Co(NO₂)₂(en)₂]Cl and 25 mL of H₂O at 50 °C was added slowly a solution of 0.189 g (0.7 mmol) of Na₂S₄O₆ in 1 mL of H₂O at 50 °C. The mixture was left stirring at 50 °C until a golden yellow solid precipitated. The solid was collected by filtration, washed with ethanol and ether and finally recrystallised from H₂O to give 0.213 g (56%) of *cis*-[Co(NO₂)₂(en)₂]S₄O₆ (**9**). δH (400 MHz, D₂O) 2.66, m, 2H, CH₂; 2.69, m, 4H, CH₂; 2.78, m, 2H, CH₂. δC (101 MHz, D₂O) 43.62; 45.35. M.p.: decomposes at 239 °C. ν_{max} 3207 cm⁻¹, 1572 cm⁻¹, 1408 cm⁻¹. *m/z* (ES): theoretical isotope model for C₄H₁₆CoN₆O₁₀S₄: 494.9 (100%); 496.9 (20.3%). Observed data: 495.1 (100%); 496.0 (10.8%). C₈H₃₂N₁₂O₁₄CoS₄: C, 12.54; H, 4.21; N, 21.61. Found: C, 12.54; H, 4.21; N, 21.93%.

2.3.10. Synthesis of *cis*-[CoCl(NH₃)(en)₂]S₄O₆ (**10**)

To a 10 mL round bottom flask was added 1.00 g (3.3 mmol) of *cis*-[CoCl(NH₃)(en)₂]Cl₂ (**1a**) dissolved in 7 mL of warm H₂O (50 °C). Then 0.95 g (3.5 mmol) of Na₂S₄O₆ dissolved in 3 mL of warm H₂O (50 °C) was added slowly. The mixture was stirred for 1 h and then left to crystallize overnight. A pink solid was collected by filtration and recrystallised from H₂O to obtain 0.37 g (25%) of *cis*-[CoCl(NH₃)(en)₂]S₄O₆ (**10**). δH (400 MHz, D₂O) 2.48, m, 2H, CH₂; 2.70, m, 4H, CH₂; 2.83, m, 2H, CH₂; 3.40, s, 0.1H, NH₃; 5.20, s, 0.1H, NH₂; 5.26, s, 0.1H, NH₂; 5.40, 2, 0.1H, NH₂. δC (101 MHz, D₂O) 44.51; 44.88; 45.10; 45.25. M.p. 185 °C. ν_{max} 3487 cm⁻¹, 3237 cm⁻¹, 3237 cm⁻¹, 1629 cm⁻¹, 1568 cm⁻¹. *m/z* (ES): Expected ions not found by ESI. C₄H₂₁N₅O₇ClCoS₄: requires C, 10.14; H, 4.47; N, 14.78. Found: C, 10.12; H, 4.37; N, 14.49%.

2.3.11. Synthesis of *cis*-[Co(ox)(en)₂]Cl · 4H₂O (**11**)

The synthesis was performed following the literature procedure [9f]. 2.85 g (10 mmol) of *cis*-[CoCl₂(en)₂]Cl was dissolved in 15 mL of hot water (60 °C). The mixture was stirred at 60 °C and when all was in solution 1.56 g (11 mmol) of (NH₄)₂ox · H₂O was added slowly. The mixture was kept stirring at 60 °C for another 30 min. Heating was stopped and the mixture was left to crystallise. *cis*-[Co(ox)(en)₂]Cl · 4H₂O was collected by filtration, washed with water, ethanol and ether to finally obtain 2.72 g (73%) **11**. δH (400 MHz, D₂O) 2.60, m, 2H, CH₂; 2.70, m, 6H, CH₂; 5.12, s, 1H, NH₂; 5.33, s, 1H. ν_{max} 3227 cm⁻¹, 3106⁻¹, 1650 cm⁻¹. M.p. 268–270 °C.

2.3.12. Synthesis of *cis*-[Co(ox)(en)₂]S₄O₆ (**12**)

To a 10 mL round bottomed flask was added 1.12 g (3 mmol) of *cis*-[Co(ox)(en)₂]Cl · 4H₂O (**11**) dissolved in

5 mL of warm H₂O (50 °C). 1.08 g (4 mmol) of Na₂S₄O₆ was then added slowly. The mixture was stirred for 2 h and then filtered. The solid was washed with ethanol and ether, then dried in air to give 0.856 g (75%) of *cis*-[Co(ox)-(en)₂]₂S₄O₆ (**12**). δ H (400 MHz, D₂O) 2.30, m, 2H, CH₂; 2.39, m, 6H, CH₂. δ C (101 MHz, D₂O) 43.42; 45.56; 167.5. M.p.: decomposes at 236 °C. *m/z* (ES): theoretical isotope model for C₆H₁₆CoN₄O₁₀S₄: 490.9 (100%); 492.9 (20.3%). Observed data: 490.9 (100%); 492.9 (25.7%). ν_{\max} 3462 cm⁻¹, 3207 cm⁻¹, 3106 cm⁻¹, 1699 cm⁻¹, 1660 cm⁻¹, 1584 cm⁻¹. C₁₂H₃₂N₈O₁₄Co₂S₄ · 15/2H₂O: requires C, 17.54; H, 4.78; N, 13.64. Found: C, 13.24; H, 4.40; N, 15.36%.

2.3.13. Synthesis of *trans*-[CoCl₂(en)₂]₂S₄O₆ (**13**)

The synthesis was performed following a procedure similar to that described in the literature for a similar system [9c]. To 1.142 g (4 mmol) of *cis*-[CoCl₂(en)₂]Cl and 18 mL of H₂O at 50 °C was slowly added a solution of 0.675 g (2.5 mmol) of Na₂S₄O₆ in 1 mL of H₂O at 50 °C. The mixture was left stirring at 50 °C for 30 min, then it was cooled in an ice bath and left to crystallise overnight. Green crystals were collected by filtration, washed with ethanol and ether to obtain 0.156 g (11%) of *trans*-[CoCl₂(en)₂]₂S₄O₆ (**13**). δ H (400 MHz, D₂O) 2.88, s, 8H, CH₂. δ C (101 MHz, D₂O) 45.27, m.p. 207–209 °C. ν_{\max} : 3230 cm⁻¹, 1226 cm⁻¹. *m/z* (ES): theoretical isotope model for C₄H₁₆Cl₂CoN₄O₆S₄: 472.9 (100%); 474.9 (83.1%); 476.9 (24.4%). Observed data: 473.0 (100%); 475.0 (94.6%); 477.2 (25.7%). Theoretical isotope model for C₄H₁₆Cl₂CoN₄: 249.0 (100%); 251.0 (64.2%); 253.0 (10.8%). Observed data: 249.0 (100%); 251.0 (64.2%); 253.0 (10.8%).

3. Results and discussion

3.1. Synthesis and reinvestigation Of [Co(en)₂(NH₃)X] and [Co(en)₂(NO₂)₂] species

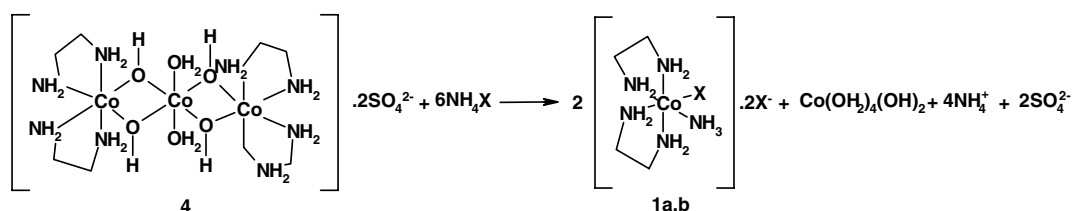
The common precursor for the [Co(en)₂(NH₃)X]²⁺2X⁻ species is the trimeric oxo-bridged complex [(Co(en)₂-μ-O₂)₂Co(H₂O)₂] · 4SO₄ (**4**) which is treated with ammonium chloride or bromide to give the analogous salts **1a,b** (Scheme 1) [10]. In these reactions a suspension of the highly insoluble trimer in water is treated with a concentrated solution of the ammonium halide, which leads to the rapid loss of the (light pink) trimer and the precipitation of the (deep purple) product. This reaction is thought

[11] to proceed via initial attack of water on the trimer (presumably at the less hindered central cobalt atom, leading to break-up of the trimer), liberating Co(en)₂ fragments which react with the ammonium halides to give the [Co(en)₂(NH₃)X]⁺ cations which precipitate as the dihalide salts. The remaining (ethylene diamine-free) cobalt ion remains in solution as an uncharacterised cobalt aqua/hydroxo complex presumably of the stoichiometry shown in Scheme 1 for charge balancing reasons. The reaction of this trimer with ammonium bromide to give **1b** has been reported to display spontaneous resolution [12], although we have been unable to reproduce this phenomenon, and have previously reported an investigation into the nature of the first formed solid product of this reaction [13]. The implications of the achirality of this structure for spontaneous resolution have been previously discussed and the structure is included here only to demonstrate that the material obtained upon recrystallisation is identical with that solved from the powder pattern of the crude reaction product. There is extensive hydrogen bonding in this material with a series of NH–Br hydrogen bonds linking complexes [13], however, here we mention only those features related to our search for conglomerate crystallisation. The metal-bound bromide has two N–H ··· Br interactions, with a neighbouring complex which is of the opposite enantiomeric configuration, one with an ethylene diamine N–H (2.575 Å) and one with an ammin N–H (2.729 Å). These interactions are mutual with the bound bromine of this complex displaying the exactly reversed hydrogen bonds. Thus the additional hydrogen bonding between counterion bromides which generate the macro-structure links together racemic pairs of complexes, hence the achiral space group (see Scheme 2).

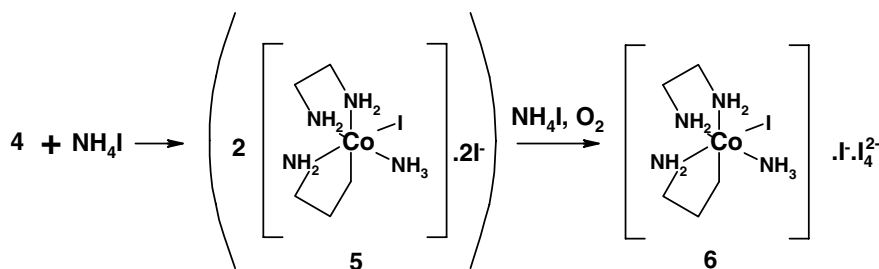
While extensive hydrogen bonding was observed in this new polymorph of this material, the interactions did not lead to conglomerate crystallisation and so other materials were examined.

As it seemed likely that other ammonium halides or pseudohalides may participate in this reaction giving similar complexes which may show hydrogen bonding in their structures and thus possibly lead to conglomerate crystallisation, the reaction of the trimer with ammonium iodide, fluoride and thiocyanate was explored.

The reaction of trimer **4** with ammonium iodide did not follow the typical course with chloride or bromide. Upon similar treatment with ammonium iodide the reaction mixture rapidly precipitated a grey-green solid, which was isolated by filtration. The mother liquor, when left to stand



Scheme 1.



Scheme 2.

slowly precipitated a very dark crystalline solid in low yield (16%), along with some excess ammonium iodide which was removed by washing with water. The initial dark grey-green solid which accounts for the mass balance of the expected cobalt species (assuming that the central cobalt of the trimer is lost) proved to be a (highly insoluble) precursor of this dark material, as attempts to characterise this initial product inevitably led to the precipitation of more of the black crystals. ¹H NMR is a useful tool in the characterisation of these complexes, as Co^{II} species are immediately identified by paramagnetic broadening, and in the (diamagnetic) Co^{III} species, *cis*- and *trans*-bis ethylene diamine complexes can easily be distinguished. The more symmetrical *trans*-complexes show broad singlets for both the methylene and amine protons, whereas in the *trans*-species each of these signals display diastereotopicity due to the metal-centred chirality, and the inequivalent methylene and amine signals are observed as complex multiplets. This black crystalline material was clearly a *cis*-Co^{III} species from the line-width and multiplicity of the proton signals, however, there were certain features such as the colour and slow formation from the mother liquor of the reaction which did not support the assignment of this material as the analogue of that obtained with iodide and bromide, i.e. [Co(en)₂(NH₃)I]2I⁻ (**5**). Crystals suitable for X-ray analysis were grown from water and the structure of the cation was confirmed as *cis*-[Co(en)₂(NH₃)I]. The expanded solid state structure of the salt is more interesting; instead of the expected iodide counterions, the charge is balanced by a mixture of isolated iodides and tetrameric iodide–iodine–iodide (I–I₂–I) chains, giving a representative formula of *cis* – [Co(en)₂(NH₃)I]₂[I⁻]₂[I₄²⁻] (**6**).

The almost perfectly linear I–I–I vector (greatest deviation 176.31°) is indicative of significant interactions between all neighbouring nuclei in the chain, and the non-symmetrical pattern of I–I lengths (I–I–I = 3.373, 2.770, 3.373 Å) suggests that I⁻–I₂–I⁻ best describes the species rather than I₄²⁻ (although this will be used hereafter as an abbreviation for this unit). The overall charge can be deduced from stoichiometry as each of the I₄ units is only half represented in the asymmetric unit, which contains one dicationic cobalt species and one isolated iodide anion. Thus each half of the I₄ chain bears a unit negative charge giving the overall I₄²⁻ formalism. Presumably the oxidation of iodide to iodine required for the formation of this prod-

uct is mediated by a Co^{III}–Co^{II} couple and aerobic oxidation, and it is this process which occurs upon standing after the initial reaction.

The space group (*P* $\bar{1}$) shows that racemic crystallisation has occurred, and thus an examination of hydrogen bonding and packing was made to see if any implications for the general model could be discerned. The packing diagram shows a double layered structure of cations separated by layers of linear [I⁻–I₂–I⁻] chains with another iodide interrupting one of the layers of cations. An investigation of close contacts (within sum of van der Waals radii) in the structure is useful for examination of the arrangements of cations in terms of their relative configurations in order to understand their packings and possibly to rationalise the formation of conglomerate and racemic structures. However, close contacts identified by this method must be treated with caution as they may not represent attractive interactions and may simply be indicative of packing arrangements. The cations are connected via three NH–I close contacts involving the (presumably) more negatively charged terminal iodides in the I₄²⁻ chains. The three contacts are between the NHs of two different ethylene diamines and an NH of the ammine ligand. The cations connected thus are of opposite absolute configuration, giving racemic crystallisation.

Each terminal I also shows close contacts to an ethylene diamine C–H (3.089 Å) and an NH (2.798 Å) of an ammine ligand in a different cation. The isolated iodide ions show close contacts with two pairs of ethylene diamine NHs, one pair each from 2 cations, and with one ethylene diamine NH and one ammine NH from a third. These cations are again of mixed absolute configuration. Finally, a contact of 3.084 Å is seen between an ethylene diamine CH and the central iodine of an I₄²⁻ unit.

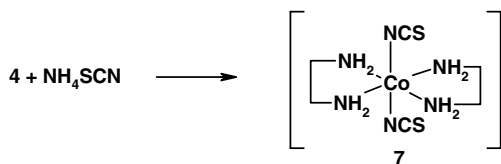
Reaction of the trimer **4** with ammonium fluoride under the standard conditions for these transformations gave an insoluble pink gum which was, surprisingly both insoluble in water (and other solvents tested) and highly hygroscopic. As it was impossible to obtain useful spectroscopic data due to the insolubility (IR was never satisfactory due to the dominant water peak) or to grow crystals due to the difficulty of dissolution, studies of this material were abandoned. The reaction with ammonium thiocyanate, however, gave a well defined solid product obtained by filtration of the reaction mixture in good yield. The IR

spectrum showed the formation of a thiocyanate complex by the clear C=N bands at 2107 cm^{-1} , however, the ^1H NMR showed only a singlet at 2.59 ppm, which is a characteristic position for ethylene diamine methylene resonances, but a multiplicity typical of a *trans*-complex. X-ray crystallography confirmed that the product was a (previously reported)[15] *trans*-[Co(en)₂SCN₂].SCN complex (7) (Scheme 3).

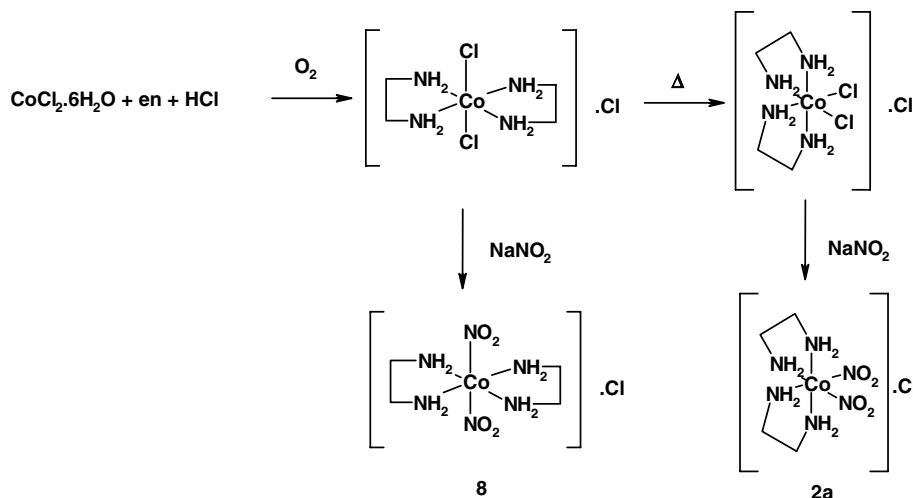
The *trans*-geometry of this product is unusual for this reaction, but only one crystal type was observed, and the NMR also indicated that the single crystal result was typical of the bulk product. Although the putative structure of the trimer is *cis*-such rearrangement of cobalt species is reasonable, especially given that the by-product of the reaction is a Co^{II} species. Assuming the possibility of rapid electron transfer between solution cobalt ions, the desired complexes have access to the geometrically labile Co^{II} state, allowing the observed isomerisation. It is worth noting, however, that this *trans*-complex has been reported to isomerise to the *cis* form on standing in water, 14 implying that the observed product is a result of crystallisation (solubility) properties.

3.2. Investigation of tetrathionate-containing structures

As the reaction of ammonium iodide, fluoride and thiocyanate with Werner's trimer 4 had failed to provide further examples of conglomerate crystallisation, attention was turned to the use of the tetrathionate anion which has been shown by Bernal to be useful in similar systems.



Scheme 3.



Scheme 4.

Sodium and potassium tetrathionate were prepared by the iodine oxidation of sodium thiosulphate, followed by salt metathesis to give the potassium salt from the mother liquor, following the literature route [9c]. An investigation was then undertaken of the structures obtained upon attempted salt metathesis of the halides of cobalt complexes with hydrogen-bonding possibilities with tetrathionate.

Bernal has rationalised the conglomerate structures obtained with tetrathionate counterions in terms of hydrogen bonding between ethylene diamine NH⁺ groups and the tetrathionate oxygen [9c]. Similarly the conglomerate structures of [Co(en)₂(NO₂)₂]₂X (X = Br, Cl) 2a,b have been rationalised in terms of hydrogen bonding between ethylene diamine NH and nitrite oxygen, and we wished to examine a combination of the effects by forming the tetrathionate salt of Co(en)₂(NO₂)₂. [Co(en)₂(NO₂)₂]₂Cl 2a was prepared by the literature method which involves the initial synthesis of [Co(en)Cl₂]₂Cl as the *trans* isomer, followed by thermal isomerisation to the *cis* species, 15 and treatment with sodium nitrite to substitute the complexed chlorides [9b]. Our initial attempt to reproduce this procedure gave, along with the desired *cis*-[Co(en)₂(NO₂)₂]₂Cl (2a), a few crystals of another green species which was identified as the (hitherto unreported) *trans*-[Co(en)₂(NO₂)₂]₂Cl (8) (Scheme 4).

Re-examination of the precursor [Co(en)Cl₂]₂Cl by ^1H NMR showed that the isomerisation had been incomplete and the bulk *cis*-species was accompanied by a small (~5%) contamination of the *trans*-isomer, explaining the origin of this undesired product. Although the crystal structure of 2a is known [8a], and the *trans* isomer 8 is non-chiral, it was of interest to examine the packing in 8 as the hydrogen bond donors and acceptors are still present. The crystals of 8 which had been obtained from the preparation of 2a were of sufficiently high quality to allow the structure to be solved by single-crystal X ray diffraction and the space group of *P21/n* confirmed that no coincidental chirality of packing had occurred. Unfortunately, the

structure proved to be a hydrate of *trans*-Co(en)₂(NO₂)₂·Cl, and this water molecule is involved in hydrogen bonding which prevents a clearer model of en-NO₂ hydrogen bonding from being obtained from this structure. The crystal structure of **8** shows no direct hydrogen bonding between complex ions, with instead hydrogen bonding between the chloride counterion and a water of crystallisation linking the cations. Each water molecule shows an O–H···Cl hydrogen bond (3.212 Å) and an O–H···O hydrogen bond (2.952 Å) to a nitrite of a complex, with the chloride showing an N–H···Cl (3.265 Å) hydrogen bond to the same complex. The water oxygen also participates in two N–H···O hydrogen bonds (3.040, 3.014 Å) with two more complexes.

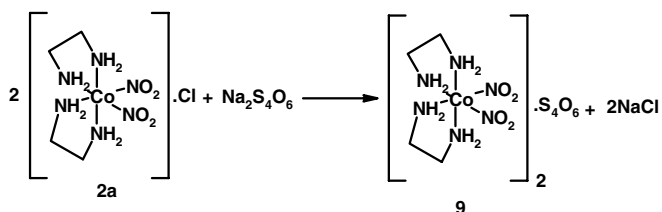
Having ensured that the sample of *cis*-Co(en)₂(NO₂)₂·Cl was homogeneous, attention returned to the salt metathesis with tetrathionate. Treatment of an aqueous solution of *cis*-Co(en)₂(NO₂)₂·Cl with aqueous sodium tetrathionate (the standard conditions for these salt metatheses) led to the precipitation of a golden-brown solid. This material was recrystallised from water to give the desired tetrathionate salt, [Co(en)₂(NO₂)₂]₂[S₄O₆] (**9**) in 55% yield (Scheme 5), and afforded some crystals suitable for single crystal X-ray diffraction.

The asymmetric unit of **9** contains two cations and a tetrathionate unit. The two cations in the asymmetric unit are of the same absolute configuration (*A* or *Δ*) and appear to be linked by hydrogen bonding with the tetrathionate (see below) thus validating the model that the chirality of a cation is transmitted into the axial chirality of the tetrathionate, and there is an ordering of the configurations of cations thus linked. The space group of the crystal, *P*21/*a*, however, indicates that the asymmetric unit is repeated by reflection through a mirror plane, and thus the overall structure is racemic. In order to understand how the initial communication of chirality through tetrathionates has failed to provide conglomerate crystallisation, an examination of the packing was undertaken. Hydrogen bonding is apparent between ethylene diamine NH and tetrathionate oxygens with each cation having two hydrogen bonds to two oxygens in a terminal SO₃²⁻ of the tetrathionate (2.915, 3.012, 2.899 and 2.947 Å). The nitrite ligands of each complex, however, form a hydrogen bond with an ethylene diamine NH in a neighbouring cation of different configuration, which uses one of its nitrites to return the bonding to an ethylene diamine NH (both 3.050 Å). Thus there is a linear arrangement with pairs of O–NH hydrogen bonds linking tetrathionate–cat-

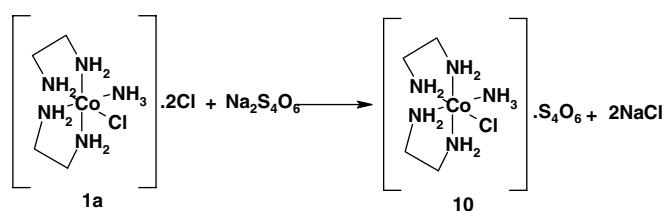
ion–cation–tetrathionate. However within this chain, the configuration alternates *P–Δ–Δ–M*. Therefore, while the strong double hydrogen bonded tetrathionate–cation successfully transmits chirality, the nitrite–NH pairing in this case inverts it. Additionally, each SO₃²⁻ also shows the oxygen not involved in the formation of the pair of hydrogen bonds to the nearest cation (in the asymmetric unit) involved in a hydrogen bonds to NHs in a cation from outside the asymmetric unit (2.969 and 2.996 Å). Again, this cation is of different configuration to those in the asymmetric unit, and itself is hydrogen bonded to a tetrathionate of a different (*M/P*) configuration to that seen in the asymmetric unit.

Thus one mechanism for the pairing of enantiomers which has now been seen twice is simple complex–complex hydrogen bonding, and thus variations in the charge of the complex (and hence the number of associated tetrathionates) and the abilities of the complex as hydrogen bond acceptors were explored. The crystallisation behaviour of the [Co(en)₂(NH₃)Cl] cation has been examined as the chloride salt [8b], but the analogous tetrathionate has not been examined. As this is a di-cationic complex, as opposed to the mono-cationic dinitrite **9** and, in the ammin ligand, has another hydrogen bond donor, we were interested to see how this change of charge and hydrogen bond donor properties could affect the interaction with the tetrathionate counterion. Salt metathesis was performed by treating [Co(en)₂(NH₃)Cl]Cl **1a** (prepared from the trimer **4**) with an equimolar quantity of aqueous sodium tetrathionate, (Scheme 6) and crystals suitable for single-crystal X-ray diffraction grown by slow evaporation of an aqueous solution.

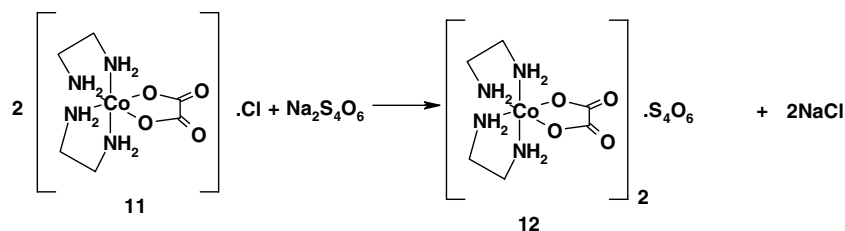
The X-ray structure confirmed the structure of the tetrathionate salt **10** but showed that it had crystallised as a mono hydrate, and indicated disorder in one of the ethylene diamine ligands. An examination of the hydrogen bonding indicated that the only multiple connection is a motif in which each end of a tetrathionate forms a hydrogen bond to the ammin group of one cation (2.943, 3.011 Å). Additionally each tetrathionate has a hydrogen bond to a water molecule (O–H···O 2.864 Å) which is additionally hydrogen bonded to an ethylene diamine in the same cation (N–H···O 2.967 Å). One of the SO₃²⁻ units of each tetrathionate shows hydrogen bonds to (2.936, 2.965 Å) two more cations, and the other SO₃²⁻ unit shows a pair of hydrogen bonds to ethylene diamine NHs in yet another cation (2.968, 2.892 Å), and an O–H···O hydrogen bond (2.904 Å) to a water molecule which acts as a bridge



Scheme 5.



Scheme 6.



Scheme 7.

to the ammine group of this same cation via an N–H···O hydrogen bond (3.308 Å).

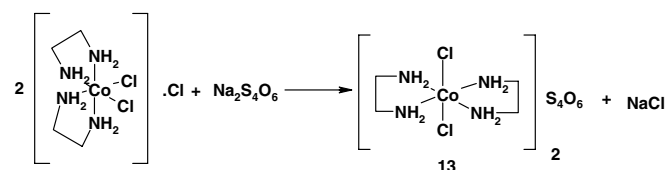
While there is extensive hydrogen bonding between cations and tetrathionates, therefore, there is no network of multiply-connected (e.g. three-point contact) entities, such as is suitable for the transmission of chirality. Most of the tetrathionate to cation hydrogen bonds are single, with many cations bonded to each tetrathionate, and also there is extensive linking through water molecules, which are not expected to transmit chirality. Thus, it is unsurprising that each tetrathionate hydrogen bonds to (connects) cations of different absolute configurations.

The use of an oxalato ligand allows another variation of the charge and hydrogen bond donor/acceptor properties, to give a mono-cationic complex with only ethylene diamine ligands capable of hydrogen bond donation, but now with hydrogen bond acceptors in the oxalato oxygens. $[\text{Co}(\text{en})_2(\text{ox})]\text{Cl}$ (**11**) was synthesised by the literature route [9f], and salt metathesis performed with a small excess of an aqueous solution of sodium tetrathionate (Scheme 7). The proton NMR confirmed that a *cis*-complex **12** had been formed, and crystals suitable for X-ray studies were grown from water. Unfortunately the crystal structure showed that, while the required compound **12** had been formed, it had crystallised as an octahydrate, with the asymmetric unit containing a single tetrathionate ion, two cations, and eight waters of crystallisation.

The space group of the structure, $P\bar{1}$, unsurprisingly, showed that the desired transmission of chirality and thus conglomerate crystallisation, had, again, failed to occur. In the presence of such extensive hydration this was to be expected, however, examination of the hydrogen bonding within the asymmetric unit was informative. The two cations in the asymmetric unit are connected by hydrogen bonds from the oxalato carboxyl oxygen to an ethylene diamine NH (2.941 Å) and the oxalato bound oxygen to another ethylene diamine NH (3.006 Å). The two cations thus linked are of the same absolute configuration, possibly hinting that such a hetero-ligand interaction could be useful in transmitting chirality. Unfortunately, the tetrathionate ions show hydrogen bonding to two different cations, of opposite absolute configuration (2.880 and 2.989 Å) and a water molecule (2.931 Å) from one SO_3^{2-} unit and from the other SO_3^{2-} unit to another two cations, again of opposite configuration (2.908, 3.030 Å), and to three water molecules (2.974, 2.879, 2.867 Å). With such extensive hydrogen bonding to water, and one point con-

tacts between tetrathionates and cations, with none of the multiple-point tetrathionate–cation contacts believed to be required for transmission of chirality, it was perhaps to be expected that racemic crystals were formed.

As a sample of *cis*- $[\text{Co}(\text{en})_2\text{Cl}_2]\text{Cl}$ had been prepared during the synthesis of **2a**, salt metathesis was attempted with this material which also represents a monocationic chiral cobalt amine complex which might show less tendency to hydration than **12**. Treatment of *cis*- $[\text{Co}(\text{en})_2\text{Cl}_2]\text{Cl}$ with sodium tetrathionate, however, gave green crystals of **13** typical of a *trans* complex (Scheme 8). Indeed, the single crystal structure of **13** proved that the *trans* isomer had been formed. This was unexpected as the sample of *cis*- $[\text{Co}(\text{en})_2\text{Cl}_2]\text{Cl}$ was believed to be homogeneous, and further investigation showed that this was indeed the case and that an isomerisation was occurring upon crystallisation as upon standing in aqueous solution the colour changed to the characteristic violet of the *cis* isomer, however, cooling or evaporation only ever gave crystals of the *trans* isomer. The reason for this isomerisation is not obvious: the reducing potential of polythionate species may allow a finite concentration of Co^{II} species to be formed and allow rapid isomerisation of the entire sample by electron transfer. The preference for crystallisation as the *trans* isomer is, presumably, a feature of packing forces. Although this *trans* isomer is achiral, an examination of hydrogen bonding was again made. The tetrathionate shows tight binding to a single cation. There is two point hydrogen bonding from one end of the tetrathionate to one cation (O–NH distances of 3.026 Å and 2.986 Å) and a single hydrogen bond to this cation from the other end of the anion (O–NH distance 2.956 Å) giving an intimate connection between the cation and anion. There are also a series of single point hydrogen bonds to other cations and the absolute configuration of the tetrathionate is inverted through a hydrogen bonded P–anion–cation–M–anion pattern with a single hydrogen bond from each end of the tetrathionates to mutually *trans*-NHs (O–NH distances 2.986 Å 2.956 Å).



Scheme 8.

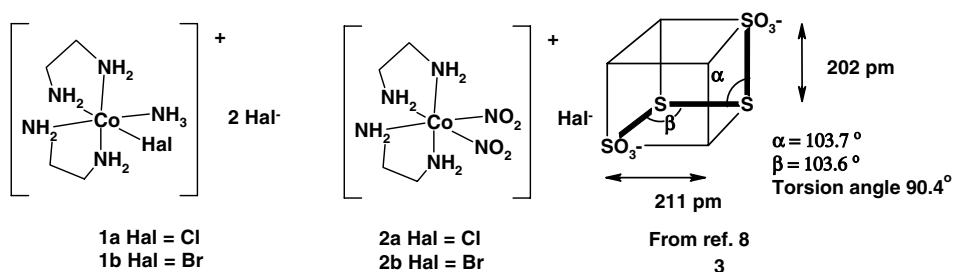
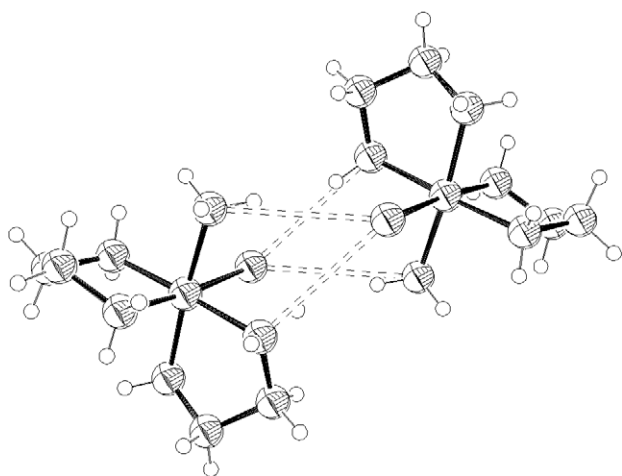
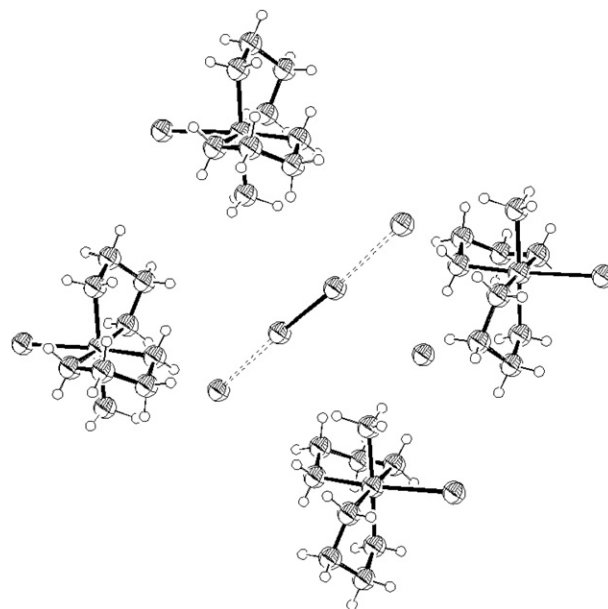
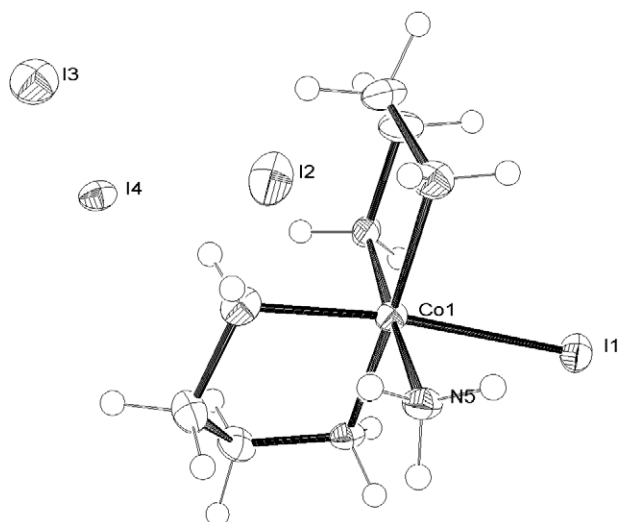
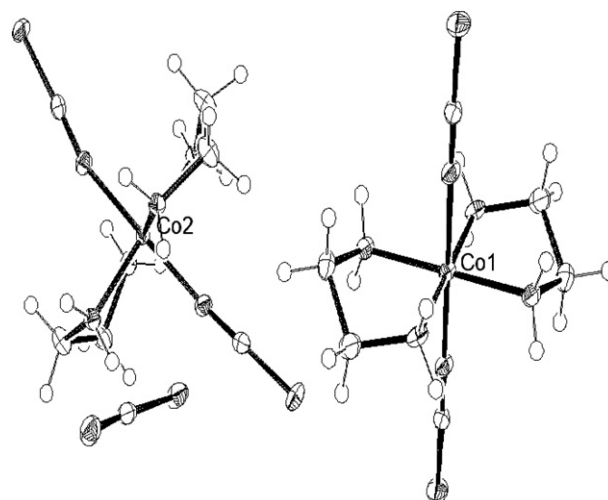


Fig. 1. Structures of Werner's complexes and tetrathionate anion.

4. Conclusions

While this search for photoracemisable materials which crystallise as conglomerates has been unsuccessful, certain hydrogen bonding patterns have been identified in $\text{Co}(\text{en})_2$

complexes, and with tetrathionates and some tentative conclusions maybe drawn as to their implications for designing conglomerate systems (see Figs. 1–16).

Fig. 2. ORTEP [14] view of **1b** hydrogen bonding leading to enantiomeric pairing.Fig. 4. ORTEP [14] view of I_4^{2-} in **6**Fig. 3. ORTEP [14] view (50% probabilities) of asymmetric unit of **6** showing half of I_4^{2-} unit.Fig. 5. ORTEP [14] view of asymmetric unit of **7**.

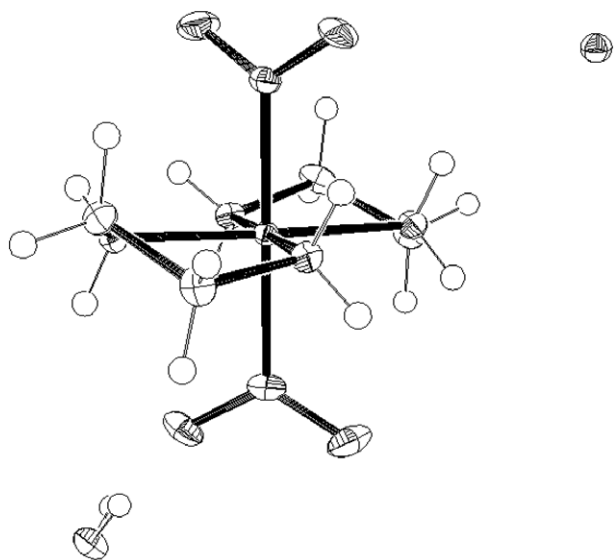


Fig. 6. ORTEP [14] view of asymmetric unit of **8** (50% probabilities).

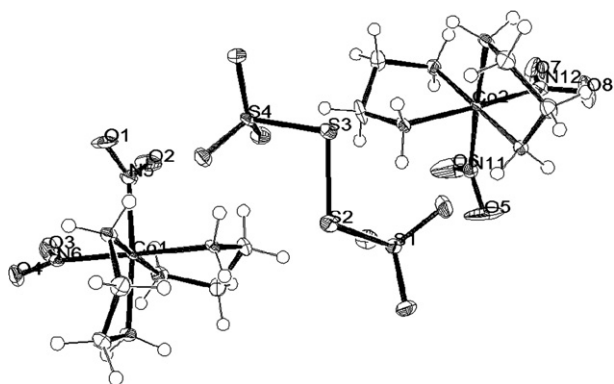


Fig. 7. ORTEP [14] view (50% probabilities) of asymmetric unit of **9**.

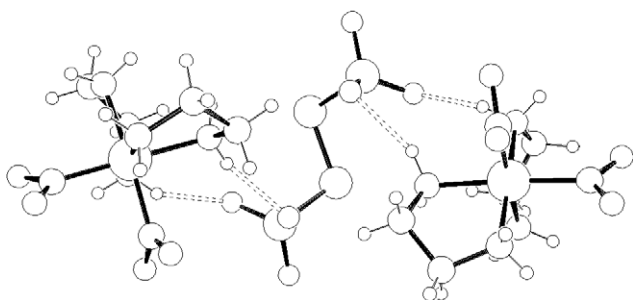


Fig. 8. Transmission of chirality in **9** through tetrathionate chains.

Firstly, there is a cation–cation mutual reciprocally paired hydrogen bond motif, in which the cations are enantiomerically paired via (en)NH–halide/oxygen H-bonds. This results in enantiomeric pairing of cations, and thus the formation of racemic crystals (**1b**, **9**, Fig. 17). Clearly this is a factor which must be controlled for any design of conglomerates based around these systems by strength-

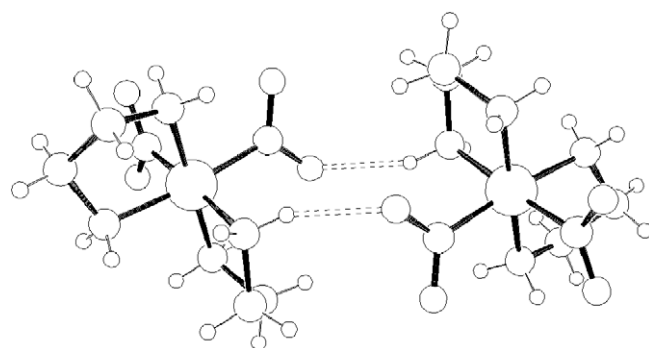


Fig. 9. Reciprocal cation–cation racemic pairing in **9**.

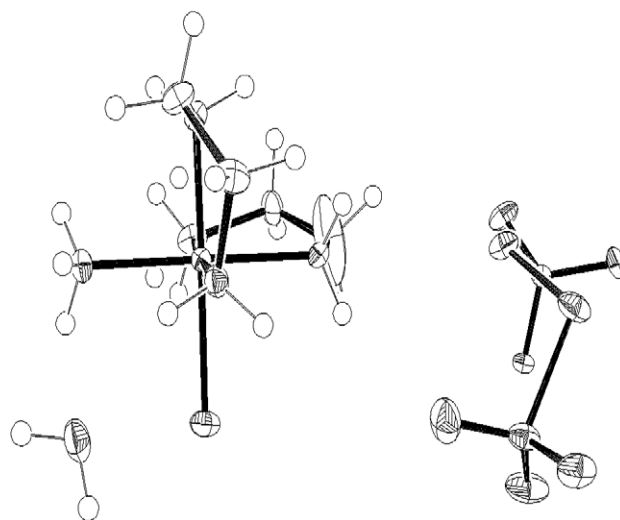


Fig. 10. ORTEP [14] view of asymmetric unit of **10** (disorder not shown).

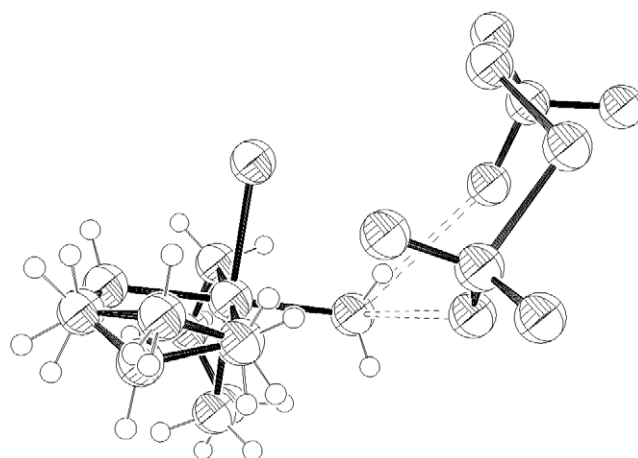


Fig. 11. Hydrogen bonding in **10**.

ening cation–anion binding to prevent this pattern from dominating. One obvious approach would be to preclude that the possibility of cation–cation hydrogen bonding would be to exclude all hydrogen bond acceptors from the structures of the cations, thus having only hydrogen

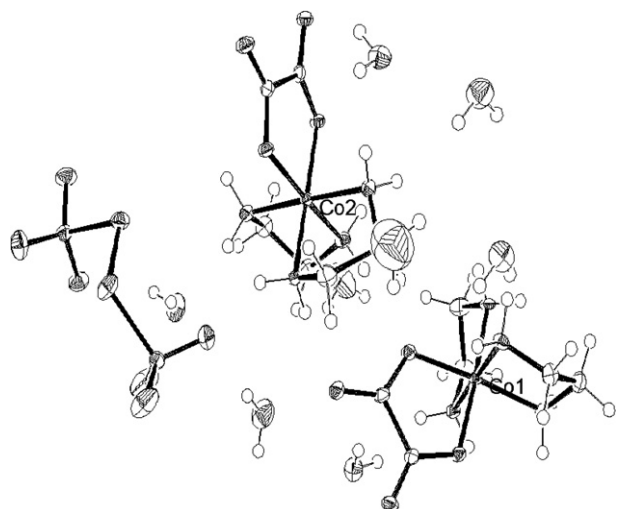


Fig. 12. ORTEP [14] view of asymmetric unit of **12** (50% probabilities).

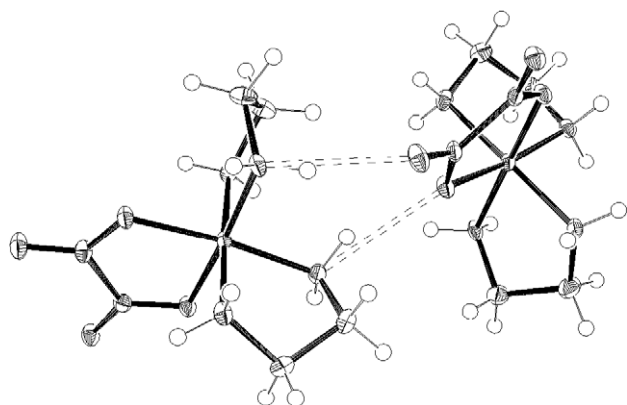


Fig. 13. Cation-cation hydrogen bonding in **12**.

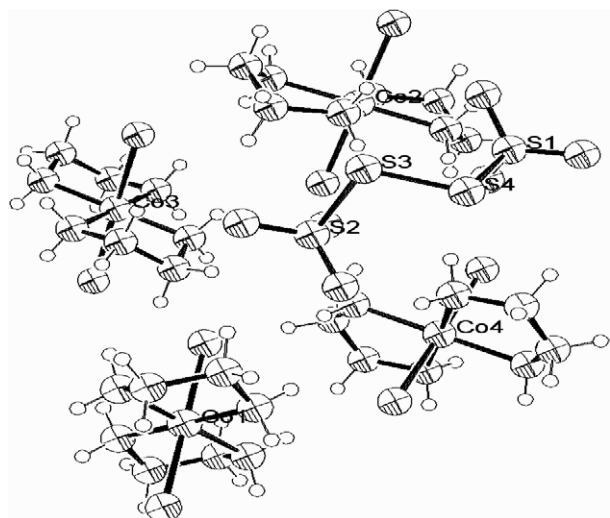


Fig. 14. ORTEP [14] view (50% probabilities) of asymmetric unit of **13** showing expanded cations (ASU contains 4×0.5 cations).

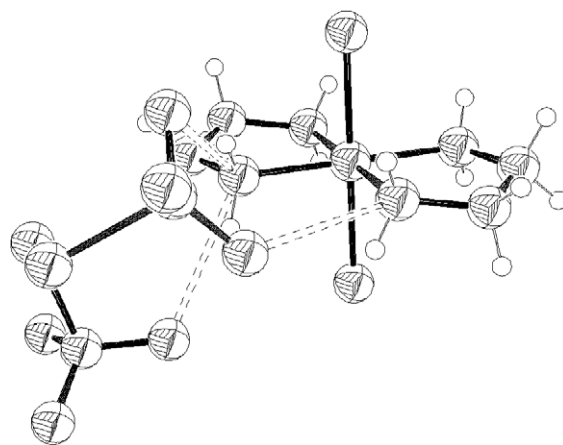


Fig. 15. Hydrogen bonding in **13**.

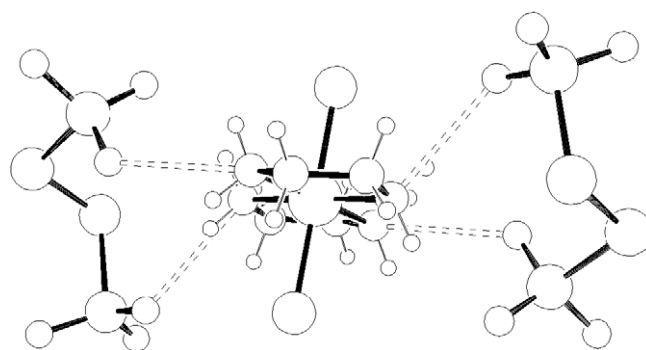


Fig. 16. Inversion of tetrathionate helicity in **13**.

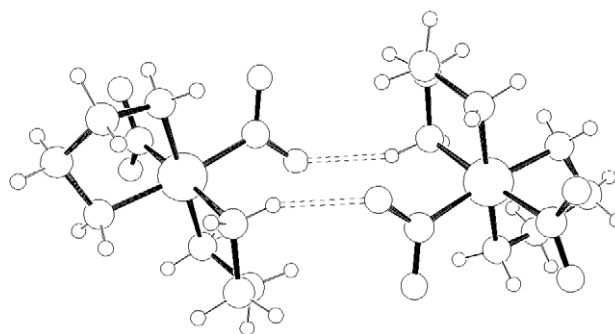
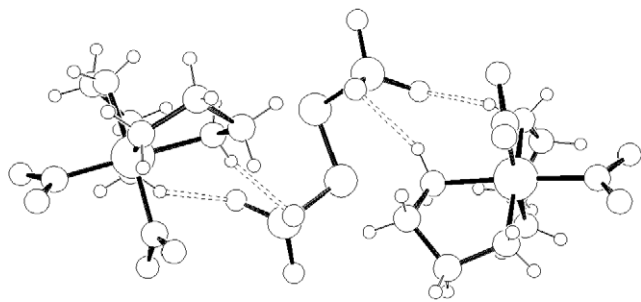
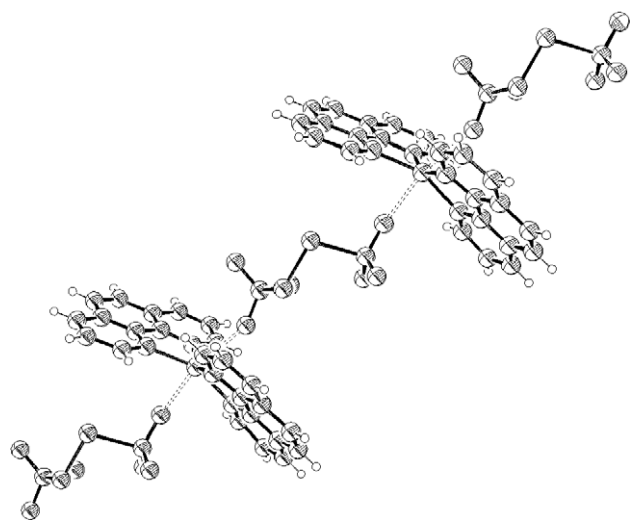


Fig. 17. Reciprocal cation-cation racemic pairing in **9**.

bonds between cations and anions. A simple possibility here was the use of $[\text{Co}(\text{en})_3]^{3+}$ as the starting material for the salt metathesis. Unfortunately, we were unable to obtain an homogeneous product or X-ray quality crystals from the reaction of such cations with potassium or sodium tetrathionate solutions.

Secondly, while we observe that the tetrathionate anion is effective in transmitting chirality through a linear double hydrogen bonded cation-tetrathionate-cation arrangement (e.g. Fig. 18), this may lead to homochiral chains of cations, packed with their enantiomeric pairs, showing a variety of cation-anion, or cation-cation hydrogen bonding

Fig. 18. Transmission of chirality in **9** through tetrathionate chains.Fig. 19. Homochiral helicate of tetrathionates in $\text{Cu}^{\text{II}}(\text{phen})_2\text{S}_4\text{O}_6^{2-}$ (ref [18]).Table 1
Selected bond lengths (Å) and angles (°) for $\text{C}_4\text{H}_{19}\text{Br}_3\text{CoN}_5$

Bond length (Å)	
Br(1)–Co(1)	2.4085(10)
Co(1)–N(5)	1.951(5)
Co(1)–N(2)	1.952(5)
Co(1)–N(3)	1.953(4)
Co(1)–N(1)	1.966(5)
Co(1)–N(4)	1.967(5)
Bond angle (°)	
N(5)–Co(1)–N(2)	177.5(2)
N(5)–Co(1)–N(3)	92.1(2)
N(2)–Co(1)–N(3)	85.4(2)
N(5)–Co(1)–N(1)	92.8(2)
N(2)–Co(1)–N(1)	89.7(2)
N(3)–Co(1)–N(1)	175.1(2)
N(5)–Co(1)–N(4)	85.56(19)
N(2)–Co(1)–N(4)	94.4(2)
N(3)–Co(1)–N(4)	90.8(2)
N(1)–Co(1)–N(4)	89.8(2)
N(5)–Co(1)–Br(1)	88.71(14)
N(2)–Co(1)–Br(1)	91.35(15)
N(3)–Co(1)–Br(1)	90.82(15)
N(1)–Co(1)–Br(1)	89.05(14)
N(4)–Co(1)–Br(1)	174.10(14)

patterns between these domains, which are inefficient at transmitting chirality and lead to racemic crystals.

It is interesting to note that this behaviour has been seen in another class of tetrathionate-containing structure. Bis-(1,10-phenanthroline) copper (II) tetrathionate [18] (Fig. 19) has a helical structure with chains of tetrathionates of the same sense of helical twist coordinating to the copper centre of cations the skew of which transmits the sense of chirality to the next tetrathionate. However, the overall structure is achiral (space group *Pbcn*) as the

Table 2
Selected bond lengths (Å) and angles (°) for $\text{C}_4\text{H}_{19}\text{CoI}_4\text{N}_5$

Bond length (Å)	
N(4)–Co(1)	1.954(6)
N(1)–Co(1)	1.966(6)
N(2)–Co(1)	1.976(6)
N(3)–Co(1)	1.980(6)
N(5)–Co(1)	1.984(5)
I(1)–Co(1)	2.6018(10)
Bond angle (°)	
N(4)–Co(1)–N(1)	90.7(2)
N(4)–Co(1)–N(2)	175.6(2)
N(1)–Co(1)–N(2)	85.1(2)
N(4)–Co(1)–N(3)	85.2(2)
N(1)–Co(1)–N(3)	91.8(2)
N(2)–Co(1)–N(3)	93.5(3)
N(4)–Co(1)–N(5)	93.3(2)
N(1)–Co(1)–N(5)	176.0(2)
N(2)–Co(1)–N(5)	90.9(2)
N(3)–Co(1)–N(5)	88.1(2)
N(4)–Co(1)–I(1)	88.34(16)
N(1)–Co(1)–I(1)	91.01(16)
N(2)–Co(1)–I(1)	93.14(18)
N(3)–Co(1)–I(1)	172.95(18)
N(5)–Co(1)–I(1)	89.56(17)

Table 3
Selected bond lengths (Å) and angles (°) for $\text{C}_4\text{H}_{18}\text{ClCoN}_6\text{O}_5$

Bond length (Å)	
Co(1)–N(2)	1.9292(18)
Co(1)–N(1)	1.9444(19)
Co(1)–N(5)	1.9484(18)
Co(1)–N(3)	1.9493(18)
Co(1)–N(6)	1.9496(18)
Co(1)–N(4)	1.9591(18)
Bond angle (°)	
N(2)–Co(1)–N(1)	179.12(8)
N(2)–Co(1)–N(5)	90.03(8)
N(1)–Co(1)–N(5)	89.09(8)
N(2)–Co(1)–N(3)	88.80(8)
N(1)–Co(1)–N(3)	91.35(8)
N(5)–Co(1)–N(3)	93.62(8)
N(2)–Co(1)–N(6)	89.14(8)
N(1)–Co(1)–N(6)	90.71(8)
N(5)–Co(1)–N(6)	86.06(8)
N(3)–Co(1)–N(6)	177.91(8)
N(2)–Co(1)–N(4)	90.40(8)
N(1)–Co(1)–N(4)	90.48(8)
N(5)–Co(1)–N(4)	179.50(8)
N(3)–Co(1)–N(4)	86.12(8)
N(6)–Co(1)–N(4)	94.21(8)

Table 4
Selected bond lengths (Å) and angles (°) for C₈H₃₂Co₂N₁₂O₁₄S₄

<i>Bond length (Å)</i>	
Co(1)–N(6)	1.915(3)
Co(1)–N(5)	1.940(3)
Co(1)–N(1)	1.948(3)
Co(1)–N(4)	1.957(3)
Co(1)–N(3)	1.979(3)
Co(1)–N(2)	1.989(3)
Co(2)–N(12)	1.928(3)
Co(2)–N(11)	1.929(3)
Co(2)–N(7)	1.951(3)
Co(2)–N(10)	1.955(3)
Co(2)–N(8)	1.979(3)
Co(2)–N(9)	1.989(3)
S(1)–S(2)	2.1170(12)
S(2)–S(3)	2.0269(12)
S(3)–S(4)	2.1171(11)
<i>Bond angle (°)</i>	
N(6)–Co(1)–N(5)	87.16(12)
N(6)–Co(1)–N(1)	93.15(12)
N(5)–Co(1)–N(1)	90.96(12)
N(6)–Co(1)–N(4)	91.54(12)
N(5)–Co(1)–N(4)	91.62(12)
N(1)–Co(1)–N(4)	174.75(12)
N(6)–Co(1)–N(3)	175.87(12)
N(5)–Co(1)–N(3)	91.12(12)
N(1)–Co(1)–N(3)	90.63(11)
N(4)–Co(1)–N(3)	84.75(11)
N(6)–Co(1)–N(2)	89.10(12)
N(5)–Co(1)–N(2)	174.43(12)
N(1)–Co(1)–N(2)	85.13(11)
N(4)–Co(1)–N(2)	92.60(12)
N(3)–Co(1)–N(2)	92.88(11)
N(12)–Co(2)–N(11)	88.83(12)
N(12)–Co(2)–N(7)	91.71(12)
N(11)–Co(2)–N(7)	90.60(12)
N(12)–Co(2)–N(10)	89.79(12)
N(11)–Co(2)–N(10)	91.15(12)
N(7)–Co(2)–N(10)	177.72(11)
N(12)–Co(2)–N(8)	91.62(12)
N(11)–Co(2)–N(8)	175.29(12)
N(7)–Co(2)–N(8)	84.71(11)
N(10)–Co(2)–N(8)	93.54(12)
N(12)–Co(2)–N(9)	173.95(12)
N(11)–Co(2)–N(9)	89.32(12)
N(7)–Co(2)–N(9)	94.07(11)
N(10)–Co(2)–N(9)	84.49(11)
N(8)–Co(2)–N(9)	90.70(11)
S(3)–S(2)–S(1)	101.94(5)
S(2)–S(3)–S(4)	101.71(5)

homochiral helices thus formed are packed along side helical chains of the opposite enantiomeric form. Thus, it is not enough for tetrathionate to chirally recognise a cation in order to cause conglomerate crystallisation, as in Co(en)₂(NH₃)Br [9c], nor even to transmit a sense of chirality between cations as in the present work and copper phenanthroline [18], as even in these cases the overall structure may be racemic. A consideration of the other nine tetrathionate-containing structures in the CCDC [19–21] gave no other examples in which tetrathionate and metal-based chirality could be related. With the exception of the Bernal structure [9c] of the tetrathionate derived from **1a**, the

Table 5
Selected bond lengths (Å) and angles (°) for C₄H₂₁ClCoN₅O₇S₄

<i>Bond length (Å)</i>	
N(3A)–Co(1)	1.958(3)
Cl(1)–Co(1)	2.2611(10)
Co(1)–N(5)	1.950(3)
Co(1)–N(2)	1.959(3)
Co(1)–N(1)	1.964(3)
Co(1)–N(4)	1.971(3)
S(1)–S(2)	2.1205(13)
S(2)–S(3)	2.0192(15)
S(3)–S(4)	2.1151(14)
<i>Bond angle (°)</i>	
N(5)–Co(1)–N(3A)	89.35(14)
N(5)–Co(1)–N(2)	89.09(13)
N(3A)–Co(1)–N(2)	94.15(13)
N(5)–Co(1)–N(1)	93.20(14)
N(3A)–Co(1)–N(1)	177.43(13)
N(2)–Co(1)–N(1)	85.50(13)
N(5)–Co(1)–N(4)	174.89(14)
N(3A)–Co(1)–N(4)	85.73(14)
N(2)–Co(1)–N(4)	92.62(13)
N(1)–Co(1)–N(4)	91.73(14)
N(5)–Co(1)–Cl(1)	89.65(10)
N(3A)–Co(1)–Cl(1)	89.53(10)
N(2)–Co(1)–Cl(1)	176.10(10)
N(1)–Co(1)–Cl(1)	90.88(9)
N(4)–Co(1)–Cl(1)	88.94(9)
S(3)–S(2)–S(1)	105.75(6)
S(2)–S(3)–S(4)	105.77(6)

Table 6
Selected bond lengths (Å) and angles (°) for C₁₂H₄₈Co₂N₈O_{21.50}S₄

<i>Bond length (Å)</i>	
Co(1)–O(11)	1.918(3)
Co(1)–O(12)	1.919(2)
Co(1)–N(11)	1.932(3)
Co(1)–N(13)	1.948(3)
Co(1)–N(14)	1.949(3)
Co(1)–N(12)	1.959(3)
Co(2)–O(21)	1.917(2)
Co(2)–O(22)	1.922(3)
Co(2)–N(23)	1.937(3)
Co(2)–N(22)	1.938(3)
Co(2)–N(24)	1.945(3)
Co(2)–N(21)	1.954(3)
S(1)–S(2)	2.1246(15)
S(2)–S(3)	2.0242(15)
S(3)–S(4)	2.1250(15)
<i>Bond angle (°)</i>	
O(11)–Co(1)–O(12)	85.32(11)
O(11)–Co(1)–N(11)	91.55(12)
O(12)–Co(1)–N(11)	175.92(13)
O(11)–Co(1)–N(13)	172.90(13)
O(12)–Co(1)–N(13)	88.37(12)
N(11)–Co(1)–N(13)	94.90(13)
O(11)–Co(1)–N(14)	90.86(13)
O(12)–Co(1)–N(14)	90.77(13)
N(11)–Co(1)–N(14)	91.89(14)
N(13)–Co(1)–N(14)	85.97(14)
O(11)–Co(1)–N(12)	90.63(13)
O(12)–Co(1)–N(12)	91.01(12)
N(11)–Co(1)–N(12)	86.39(14)

Table 6 (continued)

N(13)–Co(1)–N(12)	92.73(14)
N(14)–Co(1)–N(12)	177.76(13)
O(21)–Co(2)–O(22)	85.20(11)
O(21)–Co(2)–N(23)	175.77(13)
O(22)–Co(2)–N(23)	91.51(12)
O(21)–Co(2)–N(22)	89.02(12)
O(22)–Co(2)–N(22)	173.47(13)
N(23)–Co(2)–N(22)	94.40(14)
O(21)–Co(2)–N(24)	91.01(12)
O(22)–Co(2)–N(24)	91.04(13)
N(23)–Co(2)–N(24)	86.40(14)
N(22)–Co(2)–N(24)	92.09(14)
O(21)–Co(2)–N(21)	90.32(13)
O(22)–Co(2)–N(21)	90.73(13)
N(23)–Co(2)–N(21)	92.37(14)
N(22)–Co(2)–N(21)	86.26(14)
N(24)–Co(2)–N(21)	177.87(14)
S(3)–S(2)–S(1)	107.83(6)
S(2)–S(3)–S(4)	104.39(6)

Table 7

Selected bond lengths (Å) and angles(°) for C₈H₃₂Cl₄Co₂N₈O₆S₄

<i>Bond length (Å)</i>	
N(11)–Co(1)	1.940(4)
N(12)–Co(1)	1.962(4)
S(1)–S(2)	2.016(2)
S(1)–S(4)	2.126(2)
S(2)–S(3)	2.1315(18)
Cl(1)–Co(1)	2.2547(11)
Cl(2)–Co(2)	2.2451(12)
Cl(3)–Co(3)	2.2357(12)
Cl(4)–Co(4)	2.2627(13)
<i>Bond angle (°)</i>	
S(2)–S(1)–S(4)	105.26(8)
S(1)–S(2)–S(3)	105.35(8)
N(11)–Co(1)–N(12)	86.45(16)
N(11)–Co(1)–Cl(1)	90.48(11)
N(12)–Co(1)–Cl(1)	90.61(11)
N(21)–Co(2)–N(22)	86.01(16)
N(21)–Co(2)–Cl(2)	88.90(12)
N(22)–Co(2)–Cl(2)	90.20(12)
N(31)–Co(3)–N(32)	84.9(2)
N(31)–Co(3)–Cl(3)	90.38(13)
N(32)–Co(3)–Cl(3)	90.54(13)
N(41)–Co(4)–N(42)	86.40(16)
N(41)–Co(4)–Cl(4)	89.10(13)
N(42)–Co(4)–Cl(4)	91.11(14)

remaining structures are in achiral space groups (see Tables 1–7).

Thirdly, it is vital to ensure when trying to control crystallisation with hydrogen bond donors and acceptors that such species do not crystallise as hydrates, as water disrupts the required hydrogen bonding patterns. Therefore these complexes which are only appreciably soluble in water may not be the ideal candidates for such designs.

Acknowledgements

We wish to acknowledge The EPSRC (GR/S11480) for support, the invaluable assistance of the EPSRC national

Mass Spectrometry Service, Swansea. We also wish to acknowledge the use of the EPSRC's Chemical Database Service at Daresbury [19–21].

Appendix A. Supplementary material

CCDC 616720, 616721, 616722, 616723, 616724, 616725 and 616726 contain the supplementary crystallographic data for **1b**, **6**, **8**, **9**, **10**, **12** and **13**. These data can be obtained free of charge via <http://www.ccdc.cam.ac.uk/conts/retrieving.html>, or from the Cambridge Crystallographic Data Centre, 12 Union Road, Cambridge CB2 1EZ, UK; fax: +(44) 1223-336-033; or e-mail: deposit@ccdc.cam.ac.uk. Supplementary data associated with this article can be found, in the online version, at [doi:10.1016/j.ica.2007.06.033](https://doi.org/10.1016/j.ica.2007.06.033).

References

- [1] H.W.B. Roozeboom, Z. Physik, Chem 28 (1899) 494.
- [2] (a) R. Kuhn, Chem. Ber. 65 (1932) 49;
(b) E. Vedejs, Y. Donde, J. Am. Chem. Soc 119 (1997) 9293;
(c) E. Vedejs, R.W. Chapman, S. Lin, D.R. Powell, J. Am. Chem. Soc. 122 (2000) 3047;
(d) N.A. Hassan, E. Bayer, J.C. Jochims, J. Chem. Soc. Perkin Trans. 1 (1998) 3747;
(e) L. Czollner, W. Frantsits, B. Kuenburg, U. Hedenig, J. Frohlich, U. Jordis, Tetrahedron Lett. 39 (1998) 2087.
- [3] J.L. Bada, Nature 374 (1995) 594.
- [4] M. Avalos, R. Babiano, P. Cintas, J.L. Jimenez, J.C. Palacios, Chem. Commun. (2000) 887.
- [5] B.L. Feringa, R.A. van Delden, Angew. Chem., Int. Ed. Eng. 38 (1998) 3418.
- [6] G. Wilkinson, R.D. Gillard, J.A. McClaverty (Eds.), Comprehensive Coordination Chemistry, Vol. 4, Pergamon, 1987, p. 692, Chapter 47 (Cobalt, D.A. Buckingham and C.R. Clark).
- [7] A. Werner, On the constitution and configuration of higher-order compounds, Nobel Lecture, December 11, 1913. A. Werner and V. King, Berichte, 1911, 44, 1887.
- [8] (a) J.M. Frederiksen, E. Horn, M.R. Snow, E.R.T. Tiekink, Aust. J. Chem. 41 (1988) 1305;
(b) J. McB. Harrowfield, B.W. Skelton, A.H. White, F.R. Wilner, Aust. J. Chem. 39 (1986) 339.
- [9] (a) I. Bernal, Inorg. Chim. Acta 96 (1985) 99;
(b) I. Bernal, Inorg. Chim. Acta 96 (1985) 99;
(c) I. Bernal, J. Cetrullo, W.G. Jackson, Inorg. Chem. 32 (1993) 4098;
(d) I. Bernal, J. Cetrullo, W.G. Jackson, J. Coord. Chem. 28 (1993) 89;
(e) I. Bernal, J. Cetrullo, J. Myrcek, Mater. Chem. Phys. 35 (1993) 290;
(f) I. Bernal, J. Myrcek, J. Cai, Polyhedron 12 (1993) 1149;
(g) H. Chun, I. Bernal, Eur. J. Inorg. Chem. (1999) 717;
(h) A. Johansson, E. Wingstrand, M. Hakansson, Inorg. Chim. Acta 358 (2005) 3293.
- [10] A. Werner, A. Vilmos, Z. Anorg. Chem. 21 (1899) 145.
- [11] K. Asakura, K. Inoue, S. Osanai, D.K. Kondepudi, J. Coord. Chem. 46 (1998) 159.
- [12] K. Asakura, K. Kobayashi, Y. Mizusawa, T. Ozawa, S. Osanai, S. Yoshikawa, Physica D 84 (1995) 72.
- [13] Fang Guo, Meritxell Casadesus, Eugene Y. Cheung, Michael P. Coogan, Kenneth D.M. Harris, Chem. Commun. (2006) 1854.
- [14] ORTEP-3 for Windows L.J. Farrugia, J. Appl. Cryst. 30 (1997) 565.

- [15] Y. Liu, F.R. Fronczek, S.F. Watkins, G.W. Shaffer, R.L. Musselman, *Acta Crystallogr., Sect. C* 51 (1995) 1992.
- [16] J.C. Bailar Jr., *Inorg. Synth.* 2 (1946) 222.
- [17] H. Kobayashi, K. Ohki, I. Tsujikawa, K. Osaki, N. Uryu, *Bull. Chem. Soc. Jpn.* (1976) 49.
- [18] E. Freire, S. Baggio, R. Baggio, M.T. Garland, *Acta Crystallogr., Sect. C* 54 (1998) 464.
- [19] D.A. Fletcher, R.F. McMeeking, D. Parkin, *J. Chem. Inf. Comput. Sci.* 36 (1996) 746.
- [20] The Cambridge Structural Database F.H. Allen, *Acta Crystallogr., Sect. B* 58 (2002) 380.
- [21] ConQuest I.J. Bruno, J.C. Cole, P.R. Edgington, M. Kessler, C.F. Macrae, P. McCabe, J. Pearson, R. Taylor, *Acta Crystallogr., Sect. B* 58 (2002) 389.